American Mineralogist, Volume 74, pages 797–811, 1989

Thermally induced changes in kalsilite ($KAlSiO_4$)

CHRISTOPHER CAPOBIANCO,* MICHAEL CARPENTER
Department of Earth Sciences, Cambridge University, Cambridge CB2 3EQ, England

ABSTRACT

An experimental mineralogical investigation of the 1-atm thermal behavior of kalsilite, using TEM, high-temperature X-ray powder diffraction, and high-temperature single-crystal diffraction, revealed a previously unreported unquenchable phase for $KAlSiO_4$. This phase, $3\sqrt{3}$ kalsilite, appears stable between near 850 °C and less than 920 °C, above which characteristic superstructure diffraction effects weaken and fade into background. The high-temperature phase is a twinned pseudohexagonal phase with an orthorhombic unit cell characterized by a tripling of the room-temperature orthohexagonal dimension in the 5.16-Å hexagonal cell. TEM evidence suggests that the room-temperature phase is twinned similarly to $3\sqrt{3}$ kalsilite and might also be orthorhombic and pseudohexagonal. The transformation from kalsilite to $3\sqrt{3}$ kalsilite is thermodynamically first order in character.

High-temperature powder-diffraction results for the synthetic polymorph of $KAlSiO_4$ (O1-$KAlSiO_4$) show that the phase transition around 540 °C is characterized by continuous and dramatic increase in the c/a ratio of the orthorhombic cell. Above T_c, the c/a ratio changes insignificantly up to 1000 °C.

INTRODUCTION

Kalsilite, an uncommon rock-forming feldspathoid, occurs chiefly in K-rich, silica-undersaturated volcanic rocks. Bowen (1917) experimented with some natural specimens and concluded that $KAlSiO_4$ forms two essentially different phases. Later, Rigby and Richardson (1947) reported its artificial occurrence in the linings of a worn-out blast furnace in England. Three distinct polymorphs were recognized, and experimental studies were undertaken to sort out its polymorphic behavior. Since then, phase-equilibrium and crystallographic investigations (Smith and Tuttle, 1957; Tuttle and Smith, 1958; Cook et al., 1977; among others) have extended the list of phases at, or near, the kalsilite composition. A recent review of kalsilite mineralogy is given in Merlino (1984); ten polymorphs for this feldspathoid were noted.

Perrotta and Smith (1965) gave the first detailed single-crystal X-ray intensity analysis from a natural kalsilite and confirmed earlier work (Claringbull and Bannister, 1948) showing that kalsilite contained a tetrahedral framework structure with the tridymite topology (Fig. 1). Kalsilite is one of the classic "stuffed silica derivatives" of Buerger (1954) with K and often some minor Na as the stuffing cations. However, except for kalsilite sensu stricto, the structural details of most of the kalsilite polymorphs are not well known. It is not uncommon for kalsilite X-ray structure refinements to end up with a large R value. The residual intensity is usually attributed to oxygen sublattice disorder. Some reduction in the R value is usually achieved by creating degenerate, partially occupied sites for one or the other of the two crystallographically distinct oxygens.

Not all of the kalsilite polymorphs are stuffed tridymites. There are at least two other framework topologies reported for $KAlSiO_4$ (see Merlino, 1984). More recently, Barbier and Fleet (1988) reported on nontridymite topologies for the Ge analogue of the kalsilite composition. It is useful to group kalsilite phases according to the topology of the tetrahedral linkage because phases within such groups can be related to one another by displacive phase transitions, but only reconstructive transitions can relate phases between groups. Unfortunately, even the framework topologies of some of the kalsilite polymorphs are not known with certainty because of the lack of suitable single crystals.

All known kalsilite polymorphs are thought to have structural features in common, namely, sheets of six-membered rings of tetrahedra. This common structural feature produces a similarity of unit-cell parameters among the kalsilite polymorphs. Two sheets of tetrahedra, joined by shared apical oxygens, give the c unit-cell length of approximately 8.6 Å common to all polymorphs. The a unit-cell length is variable, but is always related in some simple geometric way to the distance between the centers of the six-membered rings of tetrahedra at approximately 5.2 Å. Differences in framework topologies are achieved by altering the sequence of up- and down-pointing tetrahedra on the hexagonal rings; this has the effect of altering the manner of linkage via the apical oxygens between the sheets. It is also worth noting in this context that recent MASNMR on several kalsilites from two

* Present address: Lunar and Planetary Laboratory, University of Arizona, Tucson, Arizona 85721, U.S.A.

0003–004X/89/0708–0797$02.00

of the topologically different groups suggests that the aluminate and silicate tetrahedra are always ordered within the three-dimensional nets (Stebbins et al. 1986).

The complexity of kalsilite mineralogy within a given framework topology arises, at least in part, from the "flexibility" of the Al–O–Si bond angles of the framework. It is now well established that a broad shallow trough exists on a plot of energy vs. hinge angle in silicate tetrahedral frameworks, e.g., Gibbs et al. (1981). Because of this "softness" in the hinge angle, the *geometrically nonrigid* frameworks are able to distort or crumple to accommodate subtle crystal-chemical influences without breaking strong Al–O or Si–O bonds. Superstructures, sometimes with large unit-cell edges, form rather easily within these materials. In kalsilite-type crystals, superstructures sometimes result from particular stuffing-cation occupancies, as in nepheline where Na and K ions in a 3:1 ratio stabilize a framework with an ordered array of two differently shaped framework cavities. Aside from the ordering of atomic species, distinct phases may also arise when these frameworks cross particular thresholds of thermal vibrational energy. The crystallographic symmetry exhibited by the framework can then change, depending on, for instance, the amplitudes of thermal motions of linking oxygens; Nukui et al. (1978) detailed such changes for tridymite.

Some of the kalsilite phases are quenchable and may be observed at room temperture; others are not. Much of the previous work on kalsilite phases was based on examination of synthetic material quenched from high temperature (e.g., Smith and Tuttle, 1957; Cook et al., 1977). Abbott (1984) reported on some high-temperature observations made on the kalsilite polymorph, kaliophilite. In this paper we have examined several kalsilites, both synthetic and natural, including a rare metamorphic sample. We present crystallographic evidence for a new unquenchable high-temperature phase of kalsilite and for the nature of phase transitions between this and other polymorphs. A phase transition in a temperature range similar to the stable temperature range of our new superstructure was previously seen in a synthetic sample by Andou and Kawahara (1982) and Kawahara et al. (1987). Additionally, we present new high-temperature crystallographic data on the structural phase transition in the so-called O1-$KAlSiO_4$ (a synthetic polymorph not having a stuffed tridymite structure). This latter transition has only been known from its lambda-type specific-heat anomaly, most recently reported by Lange et al. (1986).

Nomenclature

There seems to be no generally accepted nomenclature for the kalsilite polymorphs. Smith and Tuttle (1957) and Cook et al. (1977) identified two polymorphs produced in high-temperature synthesis as O1 and O2; only in the latter study were these phases obtained in the pure (Na-free) system. Gregorkiewitz and Schafer (1980) synthesized these same materials and referred to them as kaliophilite-O1 and kaliophilite-O2. Because kaliophilite is a naturally occurring hexagonal phase with a 27-Å unit cell, we have chosen to adopt the nonmineralogical nomenclature of Lange et al. (1986) and refer to the synthetic high-temperature orthorhombic phase as O1-$KAlSiO_4$. Below, we will present X-ray diffraction data for a phase transition in the O1-$KAlSiO_4$. The designations "high O1-$KAlSiO_4$" and "low O1-$KAlSiO_4$" would then apply.

The natural material with the smallest a unit-cell repeat (5.16 Å) is unambiguously known as kalsilite. We present diffraction data for a transition in kalsilite at magmatic temperatures that produces an orthorhombic phase with a 27-Å repeat in the unit cell. We resist calling this material kaliophilite, however, which is reserved for the hexagonal phase with $a = 27$ Å. We refer to our high-temperature kalsilite as "$3\sqrt{3}$ kalsilite" to express its unit-cell relationship with room-temperature kalsilite. We acknowledge the possibility that a stabilized, naturally occurring, low-temperature version of this material may, in fact, be kaliophilite. We also present evidence for a Na-bearing phase that for simplicity, we refer to as "$2\sqrt{3}$ kalsilite," again indicating the unit-cell relationship with kalsilite.

Note also that unless specifically qualified, diffraction indices of X-ray reflections refer to the untransformed traditional 5.16 × 8.6 Å hexagonal kalsilite cell.

Experimental methods

Starting materials

The kalsilite used in this study was obtained in several ways, with the aim of assessing behavioral differences arising from the mode of synthesis. Natural, synthetic, and ion-exchanged natural materials were examined. Sample numbers refer to the Harker collection, Department of Earth Sciences, Cambridge.

Natural samples. Kalsilite was separated from a granulite-facies emery of the Punalar district of Kerala in southern India, which was kindly provided by Dr. Michael Sandiford of the University of Adelaide, South Australia (a study on the petrogenesis of the unusual kalsilite-bearing granulite is in preparation by Sandiford and Santosh). This kalsilite was selected because (1) it contained minor Na and no Fe, as determined by electron-microprobe analysis and (2) being from a metamorphic rock, it was likely to be in the lowest structural state accessible in nature. In thin section, each large original kalsilite grain was divided into smaller domains, or subgrains; the subgrains were not in any obvious crystallographic relation to one another. This multidomain texture was not seen in any of the volcanic kalsilites examined. The composite grains were mostly disaggregated during the separation and produced material from which single crystals could be selected. This material was also used in the synthesis of O1-$KAlSiO_4$ and for ion-exchange synthesis, as described below.

Chemical analysis was made using the Cambridge Earth Sciences EDS electron microprobe. Within analytical uncertainty, the material was pure $KAlSiO_4$ and stoichio-

metric. The analysis is given in weight percent oxides as Al_2O_3 (32.674 ± 0.062); SiO_2 (38.762 ± 0.260); K_2O (29.987 ± 0.179). Subsequent electron-microprobe analysis using a wavelength-dispersive system at the University of Arizona in Tucson, Arizona, revealed a very small amount of Na. The K/Na molar ratio is near 350.

Natural nepheline from Bancroft Canada (sample no. 62015), previously characterized by Tilley (1954) and McConnell (1962), was used in this study to produce kalsilite by ion exchange. A large excess of KBr (weight ratio > 50) was added to this material and enclosed in an evacuated silica tube. The charge was held at 750 °C for 2 d, and it produced a sharp, clean, kalsilite powder-diffraction pattern. The wet-chemical analysis given by Tilley (1954) for the nepheline starting material shows a significant deviation in composition from the binary Ne-Ks join toward SiO_2. In terms of the proportions of cations and vacancies, (□), the composition is Ca:Na:K:□ = 4.9:70.7:16.4:8.0 (McConnell, 1962).

TEM observations were also made on a second metamorphic kalsilite, from Brome Mountains, Quebec (sample no. 117481). This material has been described by Philpotts et al. (1967).

Synthetic hydrothermal kalsilite. Following the methods outlined in Hamilton and Henderson (1968); a kalsilite gel was prepared from Al metal, dried K_2CO_3, and tetraethylorthosilicate. The dried, X-ray–amorphous material was placed in a Ag-Pd tube, moistened slightly with $2M$ K_2CO_3 aqueous solution, and welded shut. The capsule was held at 600 °C and 1 kbar in a standard 1-in. (2.54-cm) cold-seal bomb for 5 d. The product was fine grained with some larger crystals up to 20 μm. The larger crystals showed hexagonal outlines. The X-ray diffraction pattern yielded only sharp kalsilite peaks.

Ion-exchanged kalsilite. In addition to the pure kalsilite obtained by ion-exchanging a natural nepheline in KBr, a slightly Na-contaminated kalsilite was also obtained by ion-exchange techniques. The metamorphic kalsilite was equilibrated at 800 °C in an evacuated silica tube with a salt mixture in large excess containing 15 mol% NaBr and 85 mol% KBr. An annealing time of 1 d was sufficient to obtain crystals with a homogeneous distribution of Na as determined by electron microprobe. Electron-microprobe analysis showed that the crystals contained 4.94 ± 0.54 mol% $NaAlSiO_4$ in solid solution.

Synthetic O1-$KAlSiO_4$. This phase was obtained by annealing the metamorphic kalsilite from southern India at 1200 °C in open Pt crucibles for 2 d. After 1 d, most of the material was transformed, but 2 d were necessary for complete conversion, as gauged optically and by X-ray diffraction. Microscopically, the product consisted of the original grains as composites of many much smaller, very irregular and optically distinct domains. The most intense leucite peaks were invariably present at low intensity in diffraction patterns from the samples prepared by this method. Because of the tendency of the multidomain grains to fragment and the small subgrain size, the electron-microprobe analysis was difficult and not definitive. Nevertheless, there was no measured difference in composition between the metamorphic kalsilite and this run product. We are therefore presuming that there are no *large* departures from stoichiometry in the O1-$KAlSiO_4$ phase. Yet, the presence of leucite resulting from decomposition suggests that perhaps the high-temperature phase might be stabilized by nonstoichiometry, albeit slight. It should be noted that prolonged heating in open Pt containers at high temperature results in the total conversion of kalsilite-composition material to leucite. The nominal composition of kalsilite is $KAlSiO_4$ whereas that of leucite is $KAlSi_2O_6$.

Experimental techniques

Powder X-ray methods. For powder diffraction, a high temperature Guinier camera and programmable temperature controller (manufactured by Huber, model numbers 632 and 633, respectively) were used. The furnace was a ceramic horseshoe-type Pt resistance heater capable of temperatures to near 1000 °C. Diffraction patterns were obtained from samples held in the furnace by small loops (3 mm × 1 mm) of Pt quench wire. Two internal standards were used in heating runs: (1) Al_2O_3 powder and (2) either Al, Ag, or Au powdered metal depending on the temperature range investigated. Typically, the sample to be run was mixed in an agate mortar with a small amount of alumina and just enough glycerol to form a thick slurry. A film of the slurry was applied to the quench wire loop and held there by the surface tension of the glycerol. A tiny amount of powdered metal was then sprinkled on the wet thin film of sample plus alumina. The glycerol was evaporated at approximately 150 °C.

The spacings between nearby alumina and metal powder lines are temperature dependent and were used as internal temperature calibrations. The uncertainty in absolute temperature using this method depends on the thermal expansivity of the metal, with Al better than Ag better than Au. This sequence also corresponds to the sequence of melting points so that knowledge of the temperature is best below the melting point of Al (i.e., probably better than ±10 °C for T < 650 °C). At higher temperatures, we claim no better than ±30 °C for absolute temperatures. The relative errors in temperature for measurements within a specific heating run are, however, much better (about the ±1 °C). The relative error estimates arise from the known stability of the temperature controller and the small sample size.

The sample holder in these experiments was kept as small as possible in order to minimize temperature-gradient effects. The gradient at run conditions along the longest dimension of the sample holder was measured using miniature thermocouple probes; less than 5 °C difference was measured between the top and the bottom of the Pt loop supporting the sample.

Films were measured using a Nonius Guinier viewer permitting measurements to ±0.01°; corrections for film shrinkage were made using the alumina internal standard. Unit-cell refinements for corrected peak positions were

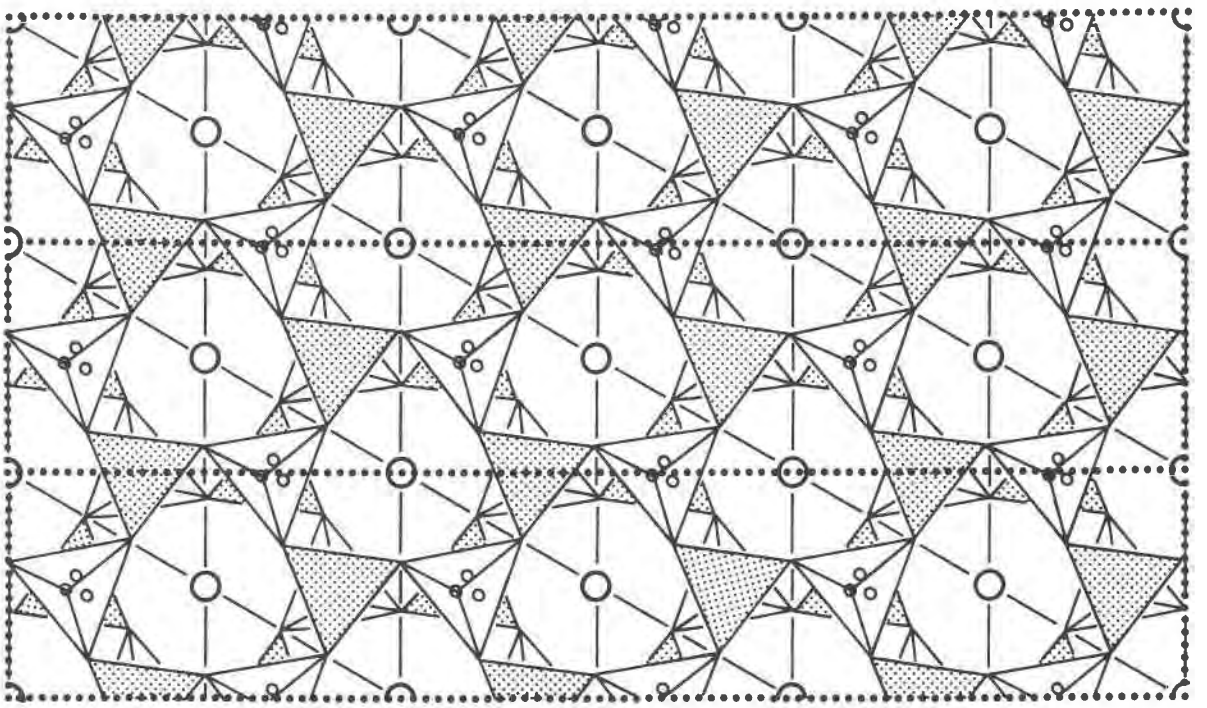

Fig. 1. Projection of the "average" kalsilite structure onto the (001) plane, after Merlino (1984); large circles are K, shaded tetrahedra are aluminate, and unshaded tetrahedra are silicate; hexagonal cell edge approximately 5.16 Å. Note that the three apical oxygens (shown as small circles on the silicate tetrahedra but also hidden beneath the aluminate tetrahedra) are in sites with ⅓ occupancy. Three cells for the new kalsilite polymorph ($3\sqrt{3}$ kalsilite) are shown by dotted lines. The framework geometry contained by the $3\sqrt{3}$ kalsilite cell will probably not show as much ditrigonal distortion because in its high-temperature stability field the structure is much expanded in the (001) plane.

calculated from a least-squares program based on that of Burnham (1962) as well as Benoit (1987).

High-temperature single-crystal X-ray methods. Single crystals for high-temperature examination were mounted inside silica capillaries that were then melted shut. To hold the crystal in place, silica glass powder was packed in behind the crystal with silica glass fibers. The fibers were left inside the capillary after sealing to serve as a pedestal for the packed glass powder and crystal. This method prevented the crystal from slipping during heat-up and therefore allowed preliminary crystal-orientation photographs to be made at room temperature.

The heater used in this apparatus was similar to the one used in the powder experiments. Although the furnace temperature was stable to ±5 °C, no attempt was made to calibrate the absolute temperature precisely during a run. Instead, preliminary series of short exposures were made with increasing power to the heater to locate the transition observed in the powder X-ray films.

Transmission electron microscopy. Kalsilite grains were gently ground under alcohol and deposited on thin C films supported by Cu grids. Several ion-thinned specimens were also prepared with the kalsilite grains mounted on Cu or Ti grids. Observations were made with an AEI EMG electron microscope operating at 100 kV. Techniques generally similar to those of Carpenter and Wennemer (1985) were adopted, using a defocused beam to reduce sample degradation. Rapid beam damage produced speckled textures in the material and resulted in diffuse diffraction patterns. The TEM observations were perforce made on grains as they lay. In the ion-thinned samples, preliminary tilting to locate a low-index reciprocal lattice plane or microstructure could be made on adjacent thinned areas before photographic exposure.

Results and interpretation

TEM observations

Kalsilite. The principal observation regarding kalsilite concerns the ubiquitous presence of polysynthetic twinning on a scale of hundreds to thousands of angstroms, as shown in Figure 2A. These twins showed black and white contrast in dark-field images obtained with reflections such as 111, 113, and 115 in **c***-[110]* sections of the metamorphic samples (Figs. 2B, 2C). Reflections of the form $\{hhl\}$ with $l = 2n + 1$ were systematically absent in diffraction patterns from some untwinned regions (Fig. 2D). In all cases the twins showed interfaces perpendicular to **c***, suggesting (001) as the composition plane. Severe (001) stacking disorder, as observed in synthetic tridymites by Carpenter and Wennemer (1985), was not observed.

Although we cannot say with absolute certainty (because of beam-damage problems) that every grain of natural kalsilite was twinned, we believe this to be the case. Significantly, the same microstructure was also observed in the kalsilites produced by other means, such as the ion-exchanged nepheline. Twinning was also seen in natural kalsilites that had been annealed at 750 °C or 950 °C under liquid KBr in evacuated silica tubes for 18 to 42 h. Only in the kalsilite hydrothermally recrystallized from a synthetic gel was no twinning observed. Notably, this latter material consisted entirely of hexagonal plates that lay preferentially with **c*** parallel to the electron beam, however. The crystals could also have been twinned, but their preferred orientation prevented unambiguous observations.

The space group $P6_3$ has been used extensively in the past for kalsilite. However, our interpretation of our TEM observations suggests that this traditional space-group assignment might be only an artifact of the ubiquitous microscopic twinning. The $P6_3$ assignment is based on the observable sixfold symmetry in the X-ray diffraction pattern coupled with systematic extinctions along **c***, specifically $00l$ with $l = 2n + 1$ absent. The same diffraction effects may also be obtained by the superposition of the diffraction patterns of orthorhombic twin domains that are stacked along **c** and rotated successively by 120° around **c**. The twin domains must be pseudohexagonal and be described by a space group that is *C*-centered and containing a *c*-guide. Such a space group is $Cmc2_1$. The $0kl$ with $l = 2n + 1$ reflections are absent in this space group, but in the twinned structure model the composite diffraction pattern would have absences only along $00l$ because the other reflections of $0Kl$ would be filled in by the other twin domains. Hence a 6_3 axis would be inferred, but only glide symmetry would exist. If kalsilite is truly orthorhombic, it must be a rather small structural detail that violates the hexad because no peak splitting was observed either in electron-diffraction patterns or in X-ray powder patterns and the refined lattice parameters were indistinguishable from hexagonal geometry.

O1-$KAlSiO_4$. Several attempts were made to examine the synthetic O1-$KAlSiO_4$ using TEM, but this material suffers even greater beam damage than the kalsilite. Nevertheless, given this rather severe limitation, no microstructure was observed. Diffraction patterns, most fairly diffuse, could be indexed using the orthorhombic cell given for O1-$KAlSiO_4$ by Cook et al. (1977). One observation of some significance was the presence of leucite in all O1-$KAlSiO_4$ material examined. The leucite grains were easily identifiable by the clarity of the grain and the twinned microstructure that showed high contrast. The observation of leucite in TEM is a confirmation of its inferred presence in all synthetic samples deduced from several weak X-ray powder-diffraction lines.

Powder diffraction

Kalsilite. For the most part, all kalsilites examined (natural, synthetic, and ion-exchanged) exhibited *qualitatively* similar diffraction effects. But, the exact temperatures at which the symmetry changes took place seemed to be sample dependent. Unfortunately, in the temperature range of interest, our temperature-calibration technique was not sufficiently accurate for us to make definitive remarks concerning the nature of the apparent absolute temperature differences between runs. A representative subset of high-temperature unit-cell-parameter data is plotted in Figures 3 and 4 illustrating the effects of thermal expansion leading to a phase transition. Complete tables of all powder-diffraction data have been deposited with the MSA data depository.[1]

There are three temperature regimes for kalsilite, low (20–850 °C), transitional (860–900 °C), and high (910–950 °C). At still higher temperatures, O1-$KAlSiO_4$ is sluggishly formed and leucite formation becomes more troublesome. We note that very weak leucite diffraction lines appear at temperatures even below the formation of O1-$KAlSiO_4$. The appearance of cubic leucite in high-temperature kalsilite diffraction patterns does not result in observable shifts in the coexisting high-temperature kalsilite line positions, suggesting that the production of leucite occurs gradually over a temperature range. When the samples are quenched to room temperature, the *c* lattice parameter for the kalsilites that have produced leucite are invariably shorter than unannealed values [compare 8.7000(10) Å for the annealed kalsilite with 8.7171(4) Å for the unannealed kalsilite], whereas the *a* parameter returns to very nearly its pre-anneal room-temperature value. The formation of leucite is irreversible and is probably a result of volatilization of K from the crystals.

Low-temperature regime. In the low-temperature regime, the kalsilite unit-cell volume undergoes an average expansion at a rate of 0.36% per 100 °C, i.e., $d(V/V_0)/dT = 36 \times 10^{-6}\ K^{-1}$. The expansion is highly anisotropic with the *c* parameter contracting by 0.06% per 100 °C, i.e., $d(c/c_0)/dT = -6 \times 10^{-6}\ K^{-1}$ and the *a* parameter expanding by 0.21% per 100 °C, i.e., $d(a/a_0)/dT = 21 \times 10^{-6}\ K^{-1}$.

An unusual effect was reproducibly observed in the low-temperature regime in the unannealed natural metamorphic sample. This effect was not seen in any of the other samples. Diffraction peaks 111, 113, and 115 are very weak in the unannealed material, but when heated to near 400 °C, the relative intensity increases irreversibly. Dollase and Freeborn (1977) noted variations in the room-temperature intensities of these same reflections in different single crystals prepared by ion exchange of natural nepheline in molten KCl. These reflections, if absent, imply the presence of a *c*-glide plane in the structure. Given the interpretation of the twinning observed by electron microscopy, it is possible that the variations are associated with variations in twin thicknesses or configurations, however. In the metamorphic sample, some partial can-

[1] A copy of the complete data set may be ordered as Document AM-89-410 from the Business Office, Mineralogical Society of America, 1625 I Street, N.W., Suite 414, Washington, D.C. 20006, U.S.A. Please remit $5.00 in advance for the microfiche.

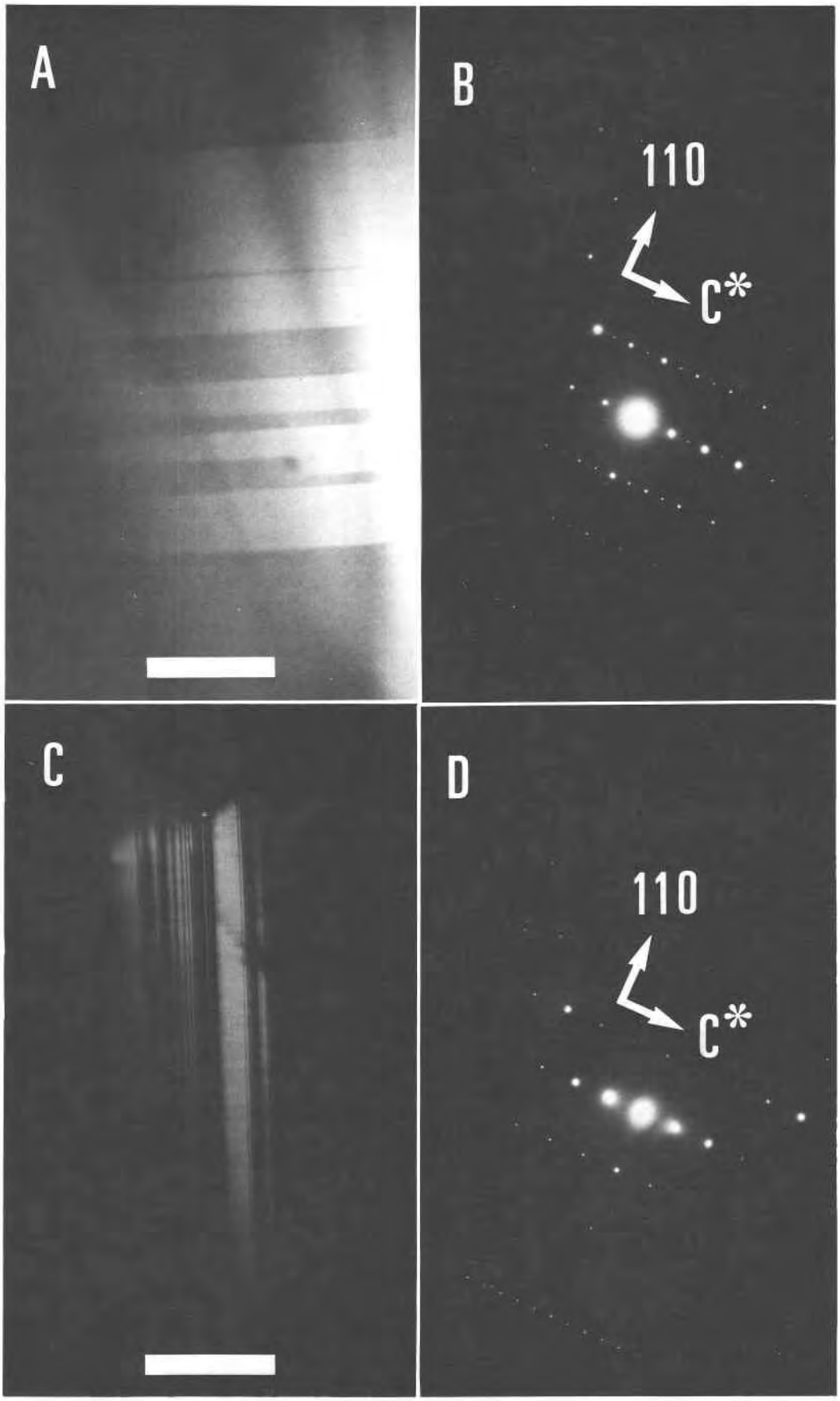
A
B
110
C*
C
D
110
C*

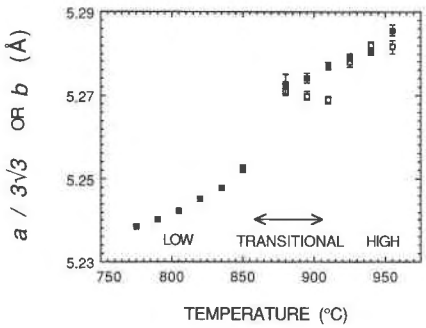

Fig. 3. Unit-cell lengths (Å) within the pseudohexagonal plane versus temperature for kalsilite. Empty square symbols for the a parameter (divided by $3\sqrt{3}$ for unit cells within and above the transition region); filled square symbols for the b parameter. Error bars are ± 1 standard error. Note that within the transition region, the a and b parameters diverge slightly, indicating *non*-pseudohexagonal dimensionality for the orthorhombic cell.

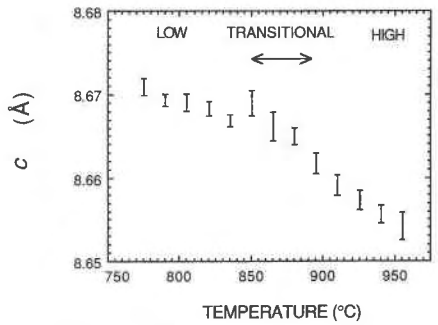

Fig. 4. Unit-cell lengths (Å) perpendicular to the pseudohexagonal plane (i.e., the c lattice parameter) versus temperature for kalsilite. Note that c decreases with temperature and is not significantly affected by the phase transition.

cellation of the X-ray intensity might result from vectorial combination of the structure factors from individual twin domains. Perhaps subsequent experimental annealing at low temperature coarsens the domains sufficiently so that the c-glide violation reflections no longer partially cancel from adjacent domains, resulting in increased intensity. Yet, it would seem that metamorphic cooling rates would produce grains as large or larger than experimental annealing. An alternative explanation is that the metamorphic kalsilite preserves a high-pressure modification that simply requires the thermal energy provided by the experimental anneal to revert to the 1-atm variety.

Transition-temperature regime. In the transition regime, occurring between 860 °C and 910 °C, new superstructure reflections appear. This is accompanied by the disappearance of the 111, 113, and 115 reflections. A list of the observed X-ray reflections from the new high-temperature phase is given in Table 1. The superstructure reflections are rather weak in the powder patterns, but their presence in the transition regime is confirmed by their reproducible appearance and disappearance during heating and cooling cycles. The new phase for kalsilite is very close to being dimensionally hexagonal, but at the low-temperature end of the range, there is some evidence that the phase becomes slightly orthorhombic (i.e., $a \neq 3\sqrt{3}b$). Reflections likely to show greatest splitting will have large components along the **a*** and **b*** axes relative to **c***. The 110 peak in low-temperature kalsilite has the largest intensity for any reflection with a zero l component. Figure 5 shows several densitometer traces over the orthorhombic 910 and the hexagonal 110 peaks. The slightly orthorhombic character of the cell in the transitional regime can be seen by a splitting of the 910 peak. In a strictly dimensionally hexagonal phase the peak would remain sharp. There is broadening in many of the other peaks with high h and k compared to l, and some of these peaks show a distinctly bimodal intensity distribution similar to that in Figure 5. In contrast, reflections with large l, for instance 004, remain sharp over the entire temperature range investigated. Figure 3 plots the b and reduced a parameters versus temperature and shows the small deviation from the metrically hexagonal cell in the transitional regime.

The transition region is complicated by the coexistence of both the superstructure phase and low-temperature phase. Figure 6 shows densitometer tracings of a larger segment of the powder pattern within the transitional region illustrating the coexistence of both phases of kalsilite over a temperature interval (the same effect is also evident in Fig. 5). The orthorhombic 910 reflection increases in intensity, and replaces the 110 reflection as more and more crystals transform. The 111 peak has no analogous reflection in $3\sqrt{3}$ kalsilite, and therefore its intensity simply decreases to zero as the proportion of transformed crystals in the powder increases. We note here that this coexistence is not due simply to kinetics because the transition is demonstrably rapid compared to the exposure times (hours) of the high-temperature X-ray exposures (see also section pertaining to single-crystal results). Furthermore, this coexistence of phases was observed in each kalsilite sample examined. Nonequilibrium coexistence by virtue of a temperature gradient within the sample was

←

Fig. 2. (**A**) Bright-field TEM micrograph of ion-thinned natural metamorphic kalsilite showing typical twin lamellae characteristic of kalsilite (scale bar approximately 0.2 μm). (**B**) (110)***-c*** R.L. plane from a twinned crystal showing the twin reflections along the **c*** direction [00l, $l = 2n + 1$ reflections are not permitted in either $P6_3$ or on (100) or (010) in orthorhombic space groups with a c-glide]. (**C**) Dark-field image obtained using an $l = 2n + 1$ reflection. (**D**) Diffraction pattern in the same orientation as that shown in 2B but from an untwinned region.

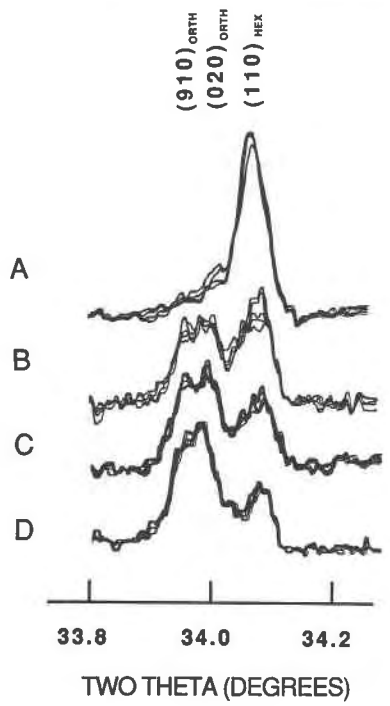

Fig. 5. Densitometer scans over a small segment of transitional-regime Guinier film exposures showing the temperature evolution of bimodal intensity for a $3\sqrt{3}$ kalsilite peak having large h and k components relative to l. Exposures A, B, C, and D are in order of increasing temperature and are separated by approximately 10 °C, except for A, which is from the low-temperature regime. The splitting of the orthorhombic peak into 910 and 020 is most easily seen in exposure C, but is barely detectible in B as well. At higher temperature (exposure D), the peaks merge and the unit cell is again dimensionally hexagonal.

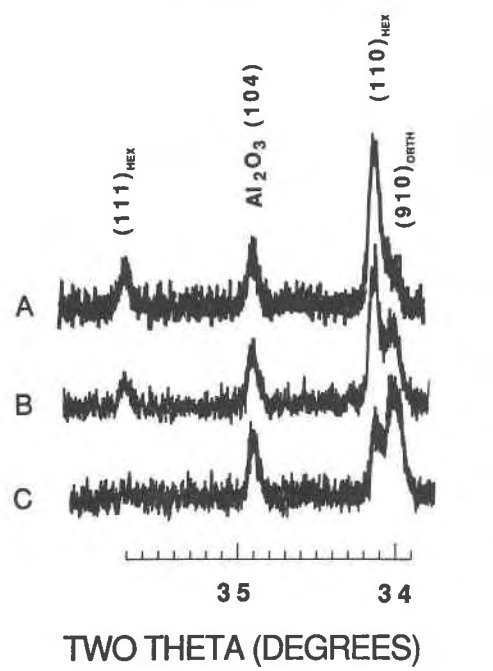

Fig. 6. Densitometer scans over a portion of high-temperature Guinier film exposures made within the transitional regime showing the coexistence of low kalsilite and $3\sqrt{3}$ kalsilite. Exposures A, B, and C are in order of increasing temperature and are separated by approximately 20 °C. The 910 peak belongs to $3\sqrt{3}$ kalsilite and increases at the expense of the 110 peak of low kalsilite. The 111 peak of low kalsilite decreases along with 110. In the transitional regime, the relative proportions of coexisting phases change with temperature.

ruled out by direct measurement of the gradient at <5 °C for the sample geometry employed.

High-temperature regime. The highest-temperature kalsilite phase observed in the powder pattern is similar to the phase reported by Andou and Kawahara (1982). By its diffraction pattern, it is essentially low-temperature kalsilite without the *hhl*, $l = 2n + 1$ reflections. We observed the $3\sqrt{3}$ superstructure lines to gradually lose their intensity and fade into background with increasing temperature. Line splitting also diminishes, and at the highest temperatures reached (ca. 910–950 °C), the phase is hexagonal and probably has the structure reported by Kawahara et al. (1987) (i.e., with an expanded framework as in the high tridymite structure). It is also in this temperature range that leucite lines in the powder pattern show increased intensity; however, they are still rather weak, and only the most intense leucite lines can be distinguished above background. It may be that the highest-temperature phase is stabilized by a small degree of nonstoichiometry resulting from the loss of the leucite component from the kalsilite.

O1-$KAlSiO_4$. Guinier powder data for the O1-$KAlSiO_4$ were collected from room temperature to around 900 °C. The patterns obtained always contained a small amount of leucite but otherwise could be indexed using the orthorhombic cell reported by Cook et al. (1977). In general, the standard errors of the refinements were larger than those in the kalsilite refinements because the O1-$KAlSiO_4$ diffraction peaks are mostly weaker and generally less sharp. At high angles, peak overlap is a serious problem. Thus, usually only ten peak positions were included in the refinement. Nevertheless, the effect of the phase transition on the lattice parameters is not obscured by these less-precise data. An apparently continuous phase transition is seen to occur near 540 °C and is characterized by a marked increase in the c unit-cell repeat. Figure 7a plots the c/a ratio versus temperature. The crystallographic effect of the phase transition is most clearly seen in this ratio, as the general thermal expansion not due to the transition is thereby removed. The b/a ratio for this material is very near $\sqrt{3}$ and is independent of temperature throughout the range investigated (see Fig. 8). This indicates that the unit cell is virtually dimensionally hexagonal above and below the transition, provided, of course, that **c** is truly perpendicular to the **a-b** plane on both sides of T_c.

Table 1. X-ray reflections observed on powder or precession photographs for pseudohexagonal $3\sqrt{3}$ kalsilite at approximately 875 °C

h	*k*	*l*	Type*	*d***	2θ†	*h*	*k*	*l*	Type*	*d***	2θ†
6	0	0	m	4.5695	19.41	2	3	1	s	1.7097	53.55
0	0	2	m	4.3275	20.51	4	3	0	s	1.7032	53.77
4	1	0	s	4.1804	21.23	15	1	1	m	1.6937	54.10
6	0	1	m	4.0409	21.98	9	1	4	m	1.6730	54.83
4	1	1	p	3.7643	23.61	4	3	1	s	1.6712	54.89
6	1	0	s	3.4539	25.77	13	2	0	s	1.6472	55.76
2	1	2	p	3.2503	27.42	6	3	0	s	1.6411	55.99
6	0	2	m	3.1421	28.38	16	1	0	s	1.6297	56.41
4	1	2	p	3.0066	29.69	6	0	5	m	1.6187	56.83
8	1	0	p, s	2.8739	31.09	13	2	1	s	1.6181	56.85
9	1	0	m	2.6380	33.95	15	1	2	m	1.6040	57.40
1	2	0	s	2.6255	34.12	12	0	4	m	1.5710	58.72
9	1	1	m	2.5234	absent	8	3	0	s	1.5645	58.99
1	2	1	s	2.5124	35.71	18	0	0	m	1.5232	60.75
6	0	3	m	2.4395	36.81	15	2	0	s	1.5023	61.69
10	1	0	p, s	2.4327	36.92	15	1	3	m	1.4818	62.64
3	2	1	s	2.4320	36.93	10	3	0	s	1.4801	62.72
5	2	0	s	2.3769	37.82	9	1	5	m	1.4472	absent
5	2	1	s	2.2920	39.27	18	0	2	m	1.4368	64.84
12	0	0	m	2.2847	39.40	12	3	0	s	1.3935	67.11
9	1	2	m	2.2525	39.99	12	0	5	m	1.3797	67.87
12	0	1	m	2.2091	40.81	17	2	0	s	1.3759	68.08
7	2	0	s	2.1878	41.23	12	2	4	m	1.3497	69.59
12	1	0	s	2.0965	43.11	18	2	0	m	1.3190	71.46
12	0	2	m	2.0204	44.82	1	4	0	s	1.3173	71.57
9	2	0	s	1.9940	45.45	14	3	0	s	1.3084	72.13
6	0	4	m	1.9556	46.39	3	4	0	s	1.3053	72.33
9	1	3	m	1.9468	absent	5	4	0	s	1.2822	73.84
14	1	0	s	1.8359	49.61	19	2	0	s	1.2659	74.95
11	2	0	s	1.8116	50.32	7	4	0	s	1.2498	76.09
12	0	3	m	1.7911	50.94	22	1	0	s	1.2128	78.85
2	3	0	s	1.7441	52.42	18	3	0	s	1.1513	83.99

* Type: m refers to main, i.e., nonsuperstructure, reflection observed in powder diffraction; s refers to superstructure reflection observed in single-crystal precession photographs; p refers to superstructure reflection observed on powder-diffraction film.

** Calculated by using $a = 27.417$, $b = 5.276$, $c = 8.655$ Å.

† Calculated for Cu$K\alpha$ = 1.5404 Å.

One can rarely prove from experimental data that a phase transition is thermodynamically continuous because discontinuities may be small compared to the experimental resolution. Nevertheless, in the case of O1-$KAlSiO_4$ there is a strong indication in our work that the transition proceeds smoothly and continuously with respect to crystallographic variations. The rapidly increasing c/a ratio below the transition and flat behavior above would be consistent with a thermodynamically continuous displacive transition. The calorimetric data of Lange et al. (1986) for O1-$KAlSiO_4$ are in accordance with the interpretation that there is a lambda-type specific-heat anomaly at 544 °C. We note that Lange et al. (1986) reported a second-phase transition for O1-$KAlSiO_4$ at 421 °C that we were unable to detect unambiguously in our lattice-parameter measurements.

We were unable to obtain suitable single crystals of the O1-$KAlSiO_4$, and therefore we cannot further address any detailed symmetry changes associated with this transition. However, we note that the powder patterns did not show any coalescence of diffraction peaks as the transition temperature was approached. Also, no observable diffraction peaks were extinguished above the transition. Nevertheless, if a *spontaneous strain* is defined in terms of the variation in c alone as

$$\epsilon_s = (c_0 - c)/c_0,$$

where c_0 is the c parameter of the high-temperature phase linearly extrapolated down to the temperature where c was measured, it is found that the data are consistent with $\epsilon_s^4 \propto (T - T_c)$ over a range of about 150 °C below T_c (Fig. 7b). In the simplest analysis, it is expected that $Q^2 \propto \epsilon_s$ will be observed for a zone-boundary transition and $Q \propto \epsilon_s$ for a zone-center transition, where Q is a macroscopic order parameter (see Carpenter, 1988, and Salje, 1988). Figure 7b might therefore imply either $Q^8 \propto T$ or $Q^4 \propto T$. Tricritical behavior, i.e., $Q^4 \propto (T - T_c)$, and saturation effects giving the leveling off below about 200 °C would provide a preferred explanation, but clearly single-crystal data are required to first establish the nature of the symmetry change.

High-temperature single-crystal diffraction

Pure natural kalsilite. Single crystals of pure kalsilite provide unequivocal diffraction effects of significance to the interpretation of powder data and TEM observations. The zero-layer **a*-b*** reciprocal-lattice plane recorded by the precession technique shows the most dramatic effects.

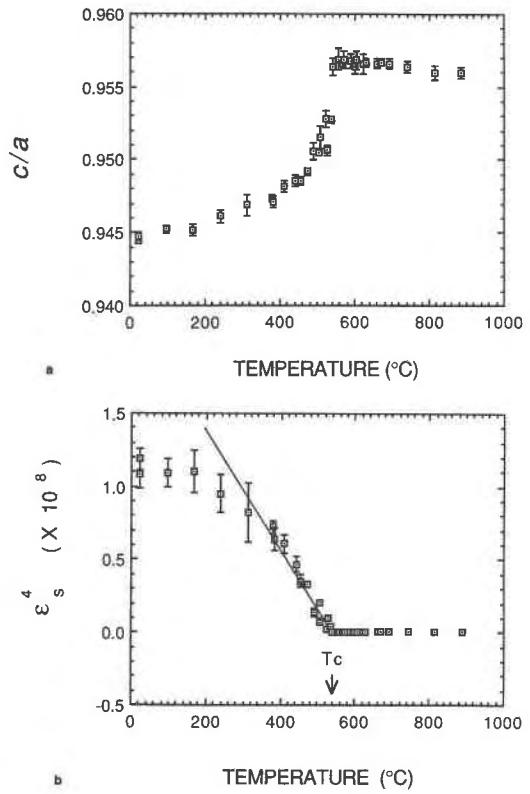

Fig. 7. (**a**) Unit-cell ratio c/a versus temperature for O1-$KAlSiO_4$ showing continuous variation with T_c near 540 °C. (**b**) The same data plotted in terms of fourth power of spontaneous strain, as defined within text.

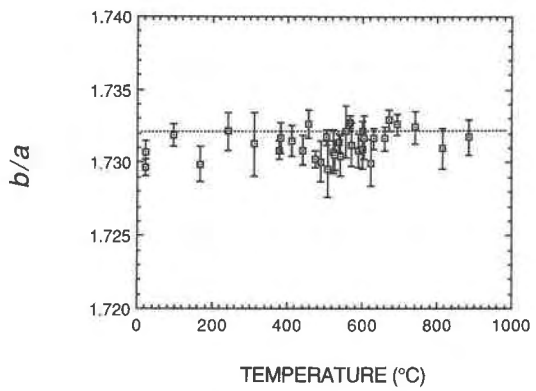

Fig. 8. Unit cell ratio b/a versus temperature for O1-$KAlSiO_4$ showing the pseudohexagonal character for both high O1-$KAlSiO_4$ and low O1-$KAlSiO_4$. Note that b/a ratio scatters around $\sqrt{3}$ as expected for an orthohexagonal cell.

On the other hand, the **a*-c*** plane does not change at the transition. Below the transition, the diffraction pattern is as shown in Figure 9A. When the transition temperature is reached, patterns similar to Figure 9B are obtained. Because the initial exposures to locate the transition are only 5 to 10 min, it is clear that the transition kinetics must be rapid. Lowering the temperature of the crystal results in the disappearance of the extra reflections. The transition can be cycled as often as desired in this manner; it is easily reversible. Exposures of several days were also performed above the transition temperature, and for pure kalsilite, no degradation of the diffraction pattern was seen; this is permissive evidence for a stability field of the high-temperature phase. However, we did not expose the crystals of the pure kalsilite to temperatures very much above the transition point because it is already known that the O1-$KAlSiO_4$ is formed at least as low as 1200 °C.

The X-ray diffraction pattern shown in Figure 9B can be interpreted as a superposition of three orthorhombic patterns (the unique portion of this pattern is schematically illustrated in Fig. 10) rotated successively by 120°. This is the same model used to account for the room-temperature electron-diffraction effects. We suggest, therefore, that the twinning observed in the TEM in the room-temperature samples is preserved above the transition temperature. The new spacing between the reflections along **a*** is in multiples of ⅙ along **a*** of the traditional low-temperature hexagonal reciprocal cell. The unit cell of the phase above the transition temperature in terms of the traditional hexagonal cell is given by

$$a_{orth} = (3\sqrt{3})a_{hex}; \qquad b_{orth} = b_{hex}; \qquad c_{orth} = c_{hex}.$$

We have observed no definite splitting of any of the reflections for any of the single crystals examined, again showing that the high-temperature phase does not deviate significantly from hexagonal lattice geometry. As noted above, our TEM observations of polysynthetic twinning on (001) suggest to us that low-temperature kalsilite is also only pseudohexagonal. The low-temperature kalsilite is C-centered, but the $3\sqrt{3}$ kalsilite with its larger unit cell is not centered. The transition therefore involves a tripling of one of the orthorhombic cell edges and an accompanying loss of C-centering. Usually, one thinks of superstructures forming when a crystal is cooled, but in kalsilite just the opposite seems to occur.

A summary of how the diffraction effects change with temperature is given in Table 2.

Na-bearing kalsilite. Single crystals of kalsilite that had previously been ion-exchanged to give a composition containing 5 mol% Na component were also examined using the high-temperature precession technique. First, the $3\sqrt{3}$ kalsilite forms just as in the pure kalsilite. However, with prolonged heat treatment, another transformation occurs. Figure 11 shows a complex diffraction pattern resulting from prolonged heating. This is interpreted as the superposition of the $3\sqrt{3}$ kalsilite diffraction pattern and the diffraction pattern of the $2\sqrt{3}$ kalsilite. The reflections of this new cell are spaced in multiples of ¼ of the traditional hexagonal unit cell. Again the (001) twinning is still preserved during this new transformation. The direct cell for the new Na-bearing high-temperature superstructure, in terms of the traditional

TABLE 2. Principal diffraction effects for pure kalsilite

High T	High kalsilite (> ca. 920 °C) hexagonal (?) similar to kalsilite (low T) except no *hhl* with $l = 2n + 1$; gradual fading of superstructure lines with concomitant increase of leucite lines in powder patterns.
Transition T	$3\sqrt{3}$ kalsilite (ca. 860–920 °C) twinned orthorhombic; loss of *C*-centering; disappearance of *hhl* with $l = 2n + 1$; weak superstructure lines; powder diffraction shows coexisting phases; first-order transition from kalsilite (low T).
Low T	Kalsilite (< ca. 860 °C) twinned orthorhombic (pseudohexagonal); *Cmc*2, (?); (001) twins.

low-temperature hexagonal cell, is

$$a_{orth} = (2\sqrt{3})a_{hex}; \quad b_{orth} = b_{hex}; \quad c_{orth} = c_{hex}.$$

It is of interest to note that we never obtained the $2\sqrt{3}$ kalsilite directly from the low-temperature phase; it seemed to always transform from the $3\sqrt{3}$ kalsilite. Furthermore, the process of transformation was not rapid. It could be sped up by increasing the temperature, but it was never instantaneous like the $3\sqrt{3}$ kalsilite. Also, once this phase formed, it was not easily reversible. Photographs taken at room temperature after having formed the $2\sqrt{3}$ kalsilite did not give sharp diffraction patterns. It is possible, and perhaps even probable, that the new phase of the Na-bearing kalsilite was stabilized as a result of minor chemical decomposition of the kalsilite (i.e., incongruent alkali volatilization) while in the $3\sqrt{3}$ phase. This, of course, would not be an easily reversible effect.

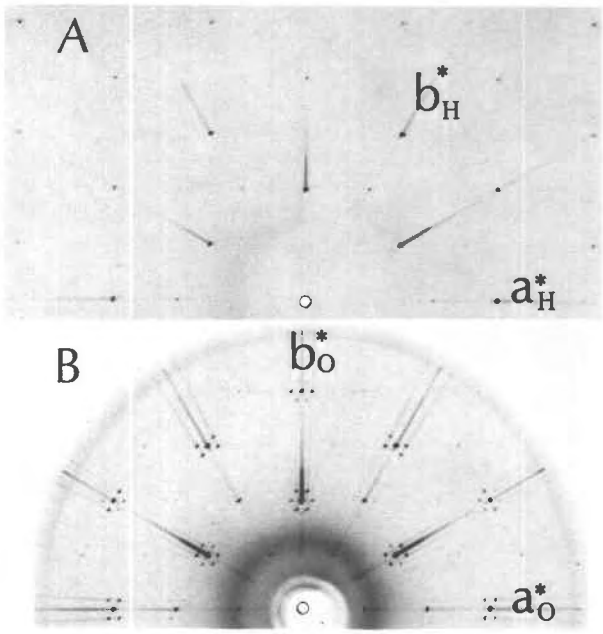

Fig. 9. **(A)** Precession photograph of the zero-layer (*hk*0) of low-temperature kalsilite. **(B)** High-temperature precession photograph for twinned $3\sqrt{3}$ kalsilite showing the superstructure reflections.

DISCUSSION

Comparison with previous work

Evidence for the $3\sqrt{3}$ kalsilite is found in the work of Kawahara et al. (1987), but it went unreported. Their high-temperature powder-diffraction patterns exhibit the weak extra reflections that are characteristic of the superstructure phase we report (weak leucite reflections are also seen). They did not index these reflections, however, and used the smaller 5.16-Å unit cell in their high-temperature, single-crystal, X-ray diffraction data collection. We have found that the superstructure phase occurs intermediately between room-temperature kalsilite and the putative fully expanded, highest-temprature phase refined by Kawahara et al. (1987). In their description of the thermal expansion of synthetic kalsilite, Henderson and Taylor (1988) also reported evidence for the onset of structural changes near 890 °C.

High-temperature studies of kalsilite polymorphs are complicated by decomposition, as noted by Abbott (1984). He investigated single crystals of a natural kaliophilite and observed no phase transitions below 850 °C. Above this temperature, his material became amorphous. This natural material was compositionally similar to our Na-containing kalsilite that we obtained by ion exchange in molten salts. Our material (containing 4.9 mol% $NaAlSiO_4$ compared to 3.9% for Abbott's material) transformed ultimately to the $2\sqrt{3}$ kalsilite at elevated temperatures but not before an intermediate step in which the $3\sqrt{3}$ kalsilite occurred. Abbott's material was apparently more susceptible than ours to thermal degradation, perhaps because of differences in experimental methods. We note that our Na-bearing material decomposed more readily than our pure K end-member and that the diffraction patterns obtained at room temperture from the former after quenching from high temperature were always of poor quality.

Twinning and phase transitions in kalsilite

The twinning in kalsilite is a ubiquitous and persistent feature of the materials examined. In pure end-member kalsilite, the twinning is carried across the phase transition into the $3\sqrt{3}$ phase. In the Na-bearing phase, it appears to persist through two phase transitions.

The volume discontinuity and the decrease in translational symmetry on heating room-temperature kalsilite into the $3\sqrt{3}$ kalsilite stability field imply that the phase transition is thermodynamically first order. The preservation of identical crystallographic axes and the twinning on both sides of the transition point indicate that the crystal-structure change cannot be too drastic, however. The preservation of the twins with interfaces parallel to (001) is probably related to the fact that both kalsilite phases, which are actually orthorhombic, are to a high degree pseudohexagonal. Because the (001) planes of both kalsilite and $3\sqrt{3}$ kalsilite have large thermal expansivities, if it were not for the nearly identical linear-expansion coefficients of a_{orth} and b_{orth} in both phases, the strain on

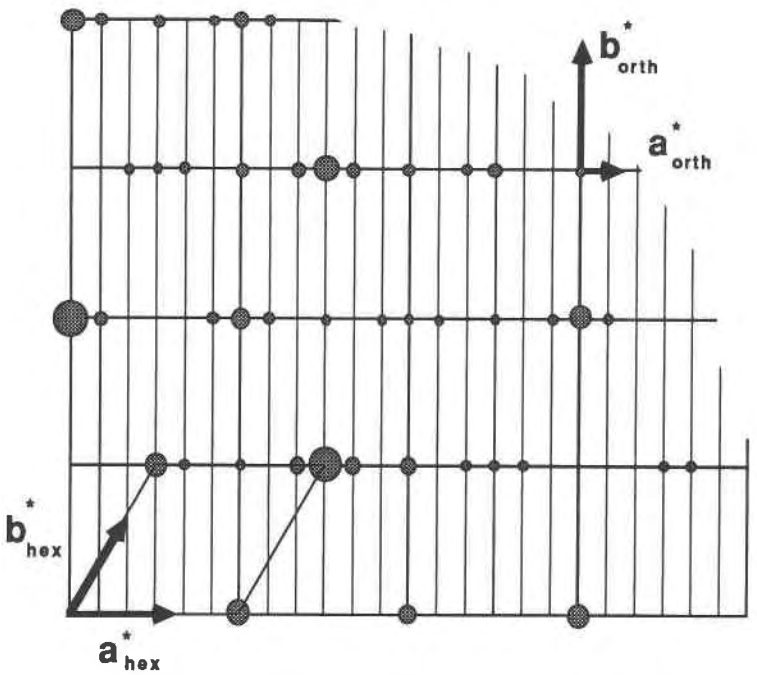

Fig. 10. Schematic diagram of one quadrant of (*hk*0) reciprocal lattice layer of the $3\sqrt{3}$ kalsilite with varying sizes of filled circles representing relative intensities. The orthorhombic cell shown as a grid is pseudohexagonal; hexagonal directions shown in diagram, with $a^*_{hex} = 6a^*_{orth}$ and $b^*_{hex} = b^*_{orth}$ (cos $\pi/6$) and, as with all kalsilite polymorphs, $c^*_{hex} = c^*_{orth}$. Superposition of three full, four-quadrant, (*hk*0) nets rotated by $2\pi/3$ produces the diffraction pattern of the twinned structure shown in the precession photograph of Fig. 9B.

the twin interface due to thermal expansion would have ruptured the coherence.

The composition plane of the twinning remains speculative, but some of the possibilities might easily be ruled out as improbable. Certainly it is possible, even in the traditional hexagonal space group $P6_3$, that a macroscopic reflection of the structure through a plane perpendicular to **c** could give the twinning observed. However, this would upset the alternating Al–O–Si linkage in the **c** direction, producing either Si–O–Si or the energetically unfavorable Al–O–Al linkage for composition planes. From their NMR data, Stebbins et al. (1986) concluded that if Si–O–Si linkages occur in the structure, they do not produce a signal strong enough to indicate the presence of planes of excess silica as a mechanism for accommodating Si in nonstoichiometric kalsilite. Dollase and Freeborn (1977) offered a plausible twinning mechanism based on the conformation of the six-membered rings of tetrahedra. Figure 1 shows the ditrigonally distorted hexagonal rings in kalsilite that all "point" in the same direction within a layer but in the opposite direction for both adjacent layers. These authors suggested a twin composition plane produced by the superposition of layers in which the ring conformation is eclipsed. This kind of twinning could be preserved during homogeneous expansion in the (001) plane and would disappear during the transformation to the fully expanded high tridymite framework topology.

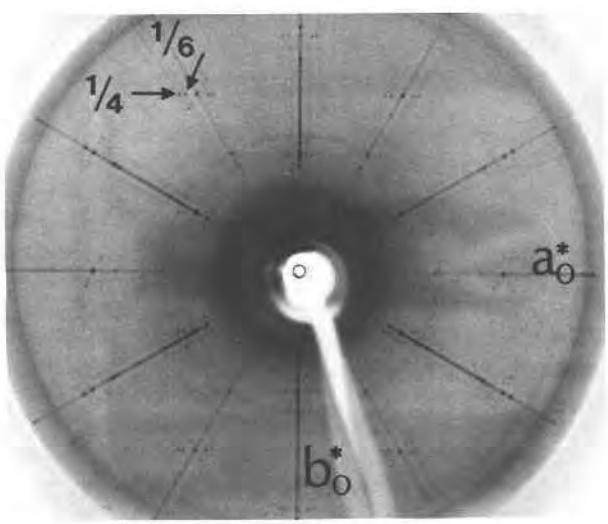

Fig. 11. High-temperature precession photograph for Na-bearing kalsilite. This complicated pattern is produced by the superposition of the precusor twinned $3\sqrt{3}$ kalsilite pattern onto the twinned $2\sqrt{3}$ kalsilite pattern that develops over time when Na is present.

An interesting feature of the transition from kalsilite to $3\sqrt{3}$ kalsilite is the apparent phase-rule violation resulting from the temperature interval of coexistence of isochemical phases. As shown in Figure 6, diffraction peaks from both phases are reproducibly found within an in-

terval of approximately 40 °C. Slow transformation kinetics were ruled out as a cause for this effect by long exposures at each temperature step as well as by the single-crystal work. A significant temperature gradient within the sample was also ruled out as a cause by direct measurement. Possible compositional differences by partial alkali volatilization were eliminated in the temperature range of interest by thermogravimetry. Similar behavior has been previously noted in tridymite-type phases. Henderson and Taylor (1982) reported the isochemical coexistence of tridymite-type phases over a temperature interval within the $(Ba,Sr)Al_2O_4$ solid solution.

One explanation of the apparent two-phase field is that it may have to do with a distribution of structural states within the powders of these chemically homogeneous samples. Because the overall free-energy change involved in the phase transitions is small, it is possible that the varying contribution of the twin-plane surface energy is enough to alter the T_c slightly. Because any twin plane is a higher-energy region compared to the untwinned region (Buerger, 1945), crystallites composed of relatively thick twin components would transform at higher temperatures than those with more narrowly spaced twin planes. This scenario differs somewhat from that suggested by Henderson and Taylor (1982) for the $(Ba,Sr)Al_2O_4$ system. They invoked "athermal" transitions wherein the extent of transformation is limited by the structural stress set up within a region of the partially transformed crystallite. Larger thermal energies and, hence, higher temperatures are then required to overcome the pinning effect. This model requires structural coherence between low- and high-temperature phases as could well be the case for the transition of room-temperature kalsilite to $3\sqrt{3}$ kalsilite. The two models differ in that the "athermal" transition would be revealed in single crystals by the superposition of the diffraction patterns of the high- and low-temperature phases over the coexistence range. In the interface-energy explanation, each crystal transforms at a specific T_c, and it is only in the bulk powder sample where the temperature range is observed. Our single-crystal results lend more support to the latter interpretation for kalsilite.

Thermal expansion in O1-$KAlSiO_4$ and kalsilite

On the basis of an unpublished single-crystal study of a synthetic and complexly twinned specimen of O1-$KAlSiO_4$ it was determined that the O1-$KAlSiO_4$ structure does not have the tridymite topology (Dr. Michael Gregorkiewitz of the Instituto de Ciencia de Materiales, Madrid, Spain, personal communication). Our new high-temperature X-ray powder data illustrate this structural difference by the marked contrast in thermal expansion behavior between tridymite- and non-tridymite-type phases. The comparison is between kalsilite and O1-$KAlSiO_4$, which have similar c lattice parameters, near 8.6 Å, corresponding in both phases to twice the thickness of a sheet of up- and down-pointing silicate and aluminate tetrahedra. The difference between the structures, relating to the linkage between the sheets, is highlighted in the thermal-expansion behavior of c. In kalsilite, c contracts, albeit slightly, as temperature increases whereas in O1-$KAlSiO_4$, the expansion between the sheets is very large and ultimately results in the observed phase transition. Conversely, the phase transition reported for kalsilite is characterized by large changes in a (i.e., the intrasheet cell dimension) whereas in O1-$KAlSiO_4$ the analogous parameter shows only modest expansion.

This study reports diffraction effects that indicate that the detailed structure of kalsilite cannot be exactly as depicted in Figure 1. However, it is also true that the actual departure is likely to be small, though not insignificant. The simple average structure shown in Figure 1 depicts the 5.16-Å cell, which contains only two crystallographically distinct oxygen atoms; the basal oxygens of the tetrahedra are symmetrically equivalent, and all apical oxygens of the tetrahedra linking the sheets are equivalent as well. In the ideal structure, i.e., the structure without any degenerate, partially occupied sites, the Si–O–Al angle that links the sheets together (the intersheet Si–O–Al angle) is constrained by the symmetry of $P6_3$ to be 180°. But single-crystal studies for kalsilite show (e.g., Perrotta and Smith, 1965; Kawahara et al., 1987) that the apical oxygens are displaced from the ideal position and assigned partially occupied, symmetrically equivalent positions. This has the effect of narrowing the intersheet hinge angle. Since the corner-sharing tetrahedral structure of kalsilite is interconnected in three dimensions, it is likely that the displacement of the apical oxygen also removes the symmetrical equivalence of the basal oxygens. The 5.16-Å cell results from a randomization of these effects. The diffraction data presented above for both kalsilite and $3\sqrt{3}$ kalsilite suggest that Figure 1 is probably oversimplified. The possibility of an ordered array of tilted tetrahedra producing the superstructure phase and even the room-temperature phase seems attractive. But in the absence of a detailed structural model for tetrahedral canting, we use the simplified 5.16-Å cell structure to qualitatively examine the highly anisotropic thermal expansion.

The 5.16-Å cell structure contains only two distinct Si–O–Al hinging angles, reflecting the approximation of two crystallographic sites for oxygen and special positions for Si and Al. Both of these angles may be approximated as a function of lattice parameters by assuming the geometrical relations among regular tetrahedra and using constant Si–O and Al–O bond lengths. The intrasheet hinge angle is then a function only of the a lattice parameter:

$$\cos \Omega_a = [a^2/3 + (1/9)(d_{Al} + d_{Si})^2 - d_{Al}^2 - d_{Si}^2]/(-2d_{Al}d_{Si}).$$

The intersheet hinge angle is a function of c:

$$\cos \Omega_c = [c^2/4 - (10/9)^2(d_{Si}^2 + d_{Al}^2)]/[(-20/9)d_{Si}d_{Al}].$$

In these geometrical equations a and c are the hexagonal unit-cell dimensions; d_{Al} and d_{Si} are the Al–O and Si–O bond lengths, respectively. At room temperature, Ω_a is

143° and Ω_e is 152°; at 850 °C the intrasheet hinge opens to 148° while the intersheet angle closes slightly to 151°. The thermal expansion in the simplified kalsilite structure tends to lessen the difference between the two average hinging angles. Totally analogous effects are described in the high-temperature structure refinement of Kawahara et al. (1987) using the 5.16-Å cell, which shows that the ditrigonal distortion of the hexagonal rings is lessened and the triply degenerate apical oxygens are forced further from their special position. However, if the apical oxygens move farther from their special positions, thus narrowing the intersheet hinge even more, it becomes even more difficult to maintain that the basal oxygens are symmetrically equivalent. It is likely that this simplified structural model does not contain enough degrees of freedom to give an accurate depiction of the situation. The conclusion is that, aside from all other diffraction effects, even the thermal expansion behavior of kalsilite suggests that the simplified 5.16-Å structure is inadequate.

It is easy to envisage ordering schemes for the displacements of the apical oxygens that, when combined with twinning on (001), would resolve many of the structural and diffraction issues. In the simplest case, all the apical oxygens would be displaced in the same directional sense. The resulting structure would be orthorhombic and could have space group $Cmc2_1$. Three twin variants would arise from a $P6_3mc$ parent structure with disordered apical-oxygen displacements. The superposition of the diffraction patterns arising from the twin domains would give an apparent space group of $P6_3$ and an average structure with three partially filled apical-oxygen sites as discussed above. Different ordering schemes can be devised to account for other superstructure types. Further structure refinements to test these possible schemes should be instructive.

Summary and concluding remarks

There have been many polymorphs reported for the compound $KAlSiO_4$. In this work, new crytallographic data (TEM observations, powder-diffraction data, and single-crystal precession data) on two varieties, kalsilite and O1-$KAlSiO_4$, are presented along with some detail on the phase transitions observed in situ. However, the study focuses on the behavior of only the naturally occurring phase, kalsilite, a member of the stuffed-silica-derivative family of crystal structures.

Much of the mineralogical complexity exhibited by kalsilite can probably be traced to the unfavorable Si–O–Al angle of 180° imposed by the ideal kalsilite structure along the hexagonal **c** axis. Effects reported within this work can be related to structural adjustments of the framework to find more favorable polyhedral hinge angles. However, we note that further structural characterization will be required to interpret quantitatively some of the following general features: (1) Twinning in kalsilite is endemic. The details of the traditional kalsilite structure (see Fig. 1) are probably due to the diffraction effects caused by the superposition of microscopic twins. (2) A new high-temperature and unquenchable phase for kalsilite ($3\sqrt{3}$ kalsilite) is sensitive to the pre-existing microstructural state within the low-temperature phase. Specifically, the equilibrium transition temperature may depend on the extent of twinning. (3) Thermal expansion within kalsilite is highly anisotropic. Similar anisotropy has also been reported in other kalsilite-type phases, e.g., $KFeSiO_4$ (Bentzen, 1983), perhaps testifying only to the easy collapsibility within the plane perpendicular to **c**. (4) The effect of minor-element contamination on the behavior is pronounced. A new high-temperature phase ($2\sqrt{3}$ kalsilite) was produced by adding a little Na (approximately 5 mol%) to pure kalsilite. The transition sequence with increasing temperature is kalsilite to $3\sqrt{3}$ kalsilite to $2\sqrt{3}$ kalsilite. The last transition in the sequence occurs rather slowly, suggesting the possibility that order-disorder among the alkalis within the framework cavities might be playing a significant role, as in nepheline, thus permitting still other stabilizing framework adjustments. Alternatively, framework adjustments yielding $2\sqrt{3}$ kalsilite might be induced by nonstoichiometry produced by slight high-temperature decomposition.

Acknowledgments

This work was supported by a NATO postdoctoral fellowship awarded to C.C. in March 1986 and by the resources of the Department of Earth Sciences of Cambridge University. We thank Dr. Michael Sandiford and Dr. Anthony Philpotts for providing kalsilite-bearing material for this study.

References cited

Abbott, R.N., Jr. (1984) $KAlSiO_4$, stuffed derivatives of tridymite: Phase relationships. American Mineralogist, 69, 449–457.

Andou, Y., and Kawahara, A. (1982) The existence of high-low inversion point of kalsilite. Mineralogical Journal, 11, 72–77.

Barbier, J., and Fleet, M.E. (1988) Investigation of phase relations in the $(Na,K)AlGeO_4$ system. Physics and Chemistry of Minerals, 16, 276–285.

Benoit, P.H. (1987) Adaptation to microcomputer of the Appleman-Evans program for indexing and least squares refinement of powder-diffraction data for unit-cell dimensions. American Mineralogist, 72, 1018–1019.

Bentzen, J. (1983) Three crystalline polymorphs of $KFeSiO_4$, potassium ferrisilicate. Journal of the American Ceramic Society, 66, 475–479.

Bowen, N.L. (1917) The sodium-potassium nephelites. American Journal of Science, 43, 115–132.

Buerger, M.J. (1945) The genesis of twin crystals. American Mineralogist, 30, 469–482.

——— (1954) The stuffed derivatives of the silica structures. American Mineralogist, 39, 600–614.

Burnham, C.W. (1962) Lattice constant refinement. Carnegie Institution of Washington Yearbook, 61, 132–135.

Carpenter, M.A. (1988) Thermochemistry of aluminum/silicon ordering in feldspar minerals. In E.K.H. Salje, Ed., Physical properties and thermodynamic behavior of minerals. NATO ASI series C, 225, p. 265–323. D. Reidel Publishing Company, Dordrecht, The Netherlands.

Carpenter, M.A., and Wennemer, M. (1985) Characterization of synthetic tridymites by transmission electron microscopy. American Mineralogist, 70, 517–528.

Claringbull, G.F., and Bannister, F.A. (1948) The crystal structure of kalsilite. Acta Crystallographica, 1, 42.

Cook, L.P., Roth, R.S., Parker, H.S., and Negas, T. (1977) The system K_2O-Al_2O_3-SiO_2. Part 1. Phases on the $KAlSiO_4$-$KAlO_2$ join. American Mineralogist, 62, 1180–1190.

Dollase, W.A., and Freeborn, W.P. (1977) The structure of $KAlSiO_4$ with $P6_3mc$ symmetry. American Mineralogist, 62, 336–340.

Gibbs, G.V., Meagher, E.P., Newton, M.D., and Swanson, D.K. (1981) A comparison of experimental and theoretical bond length and angle variations for minerals, inorganic solids, and molecules. In A. Navrotsky and M. O'Keefe, Eds., Structure and bonding in crystals, p. 195–225. Academic Press, New York.

Gregorkiewitz, M., and Schafer, H. (1980) The structure of $KAlSiO_4$–kaliophilite 01: Application of the subgroups-supergroups relations to the quantitative space group determination of pseudosymmetric crystals. Sixth European Crystallographic Meeting, Barcelona, July 28–August 1, Abstract, p. 155.

Hamilton, D.L., and Henderson, C.M.B. (1968) The preparation of silicate compositions by a gelling method. Mineralogical Magazine, 36, 832–838.

Henderson, C.M.B., and Taylor, D. (1982) The structural behaviour of the nepheline family: (1) Sr and Ba aluminates (MAl_2O_4). Mineralogical Magazine, 45, 111–127.

——— (1988) The structural behavior of the nepheline family: (3) Thermal expansion of kalsilite. Mineralogical Magazine, 52, 708–711.

Kawahara, A., Andou, Y., Marumo, F., and Okuno, M. (1987) The crystal structure of high temperature form of kalsilite ($KAlSiO_4$) at 950 °C. Mineralogical Journal, 13, 260–270.

Lange, R.A., Carmichael, I.S.E., and Stebbins, J.F. (1986) Phase transitions in leucite ($KAlSi_2O_6$), orthorhombic $KAlSiO_4$, and their iron analogues ($KFeSi_2O_6$, $KFeSiO_4$). American Mineralogist, 71, 937–945.

McConnell, J.D.C. (1962) Electron-diffraction study of subsidiary maxima of scattered intensity in nepheline. Mineralogical Magazine, 33, 114–124.

Merlino, S. (1984) Feldspathoids: Their average and real structures. In W.L. Brown, Ed., Feldspars and feldspathoids. NATO ASI series C 137, p. 435–470. Reidel, Dordrecht, The Netherlands.

Nukui, A., Nakazawa, H., and Akao, M. (1978) Thermal changes in monoclinic tridymite. American Mineralogist, 63, 1252–1259.

Perrotta, A.J., and Smith, J.V. (1965) The crystal structure of kalsilite, $KAlSiO_4$. Mineralogical Magazine, 35, 588–595.

Philpotts, A.R., Pattison, E.F., and Fox, J.S. (1967) Kalsilite, diopside and melilite in a sedimentary xenolith from Brome Mountain, Quebeck. Nature, 214, 1322–1323.

Rigby, G.R., and Richardson, H.M. (1947) The occurrence of artificial kalsilite and allied potassium aluminium silicates in blast-furnace linings. Mineralogical Magazine, 28, 75–89.

Salje, E. (1988) Structural phase transitions and specific heat anomalies. In E.K.H. Salje, Ed., Physical properties and thermodynamic behavior of minerals. NATO ASI series C, 225, p. 265–323. D. Reidel, Dordrecht, The Netherlands.

Smith, J.V., and Tuttle, O.F. (1957) The nepheline-kalsilite system: I. X-ray data for the crystalline phases. American Journal of Science, 255, 282–305.

Stebbins, J.F., Murdoch, J.B., Carmichael, I.S.E., and Pines, A. (1986) Defects and short-range order in nepheline group minerals: A silicon-29 nuclear magnetic resonance study. Physics and Chemistry of Minerals, 13, 371–381.

Tilley, C.E. (1954) Newpheline-alkali feldspar paragenesis. American Journal of Science, 252, 65–75.

Tuttle, O.F., and Smith, J.V. (1958) The nepheline-kalsilite system: II. Phase relations. American Journal of Science, 256, 571–589.

Manuscript received January 30, 1989
Manuscript accepted March 16, 1989